JOURNAL OF MATERIALS SCIENCE 37 (2002) 2635–2644

Plastic deformation of EVA, EVOH and their multilayers

V. GAUCHER-MIRI
Department of Macromolecular Science and Center for Applied Polymer Research, Case Western Reserve University, Cleveland, OH 44106-7202, USA

G. K. JONES, R. KAAS
Technical Center, Pechiney Plastic Packaging, Inc., Neenah, WI 54957-0702, USA

A. HILTNER*, E. BAER
Department of Macromolecular Science and Center for Applied Polymer Research, Case Western Reserve University, Cleveland, OH 44106-7202, USA

The high strain rate, plastic deformation of multilayer films is analyzed in relation to the tensile properties of the components. The multilayers combine ethylene-vinyl acetate (EVA) blend surface-layers with an ethylene-vinyl alcohol (EVOH) core-layer; the volume of the EVOH layer is varied from 1% to 20%. Individually, the components exhibit markedly different tensile behavior in terms of yielding and ductility in the temperature range from 55°C to 95°C. The EVA blend deforms homogeneously whereas EVOH forms a neck at an extension rate of 10,000%/min. It is shown that the true stress-strain relationship of the components in the plastic region can be described with two parameters, the true yield stress and the strain hardening parameter. Multilayers deform homogeneously, as does the EVA blend. A simple rule of mixtures approach is used to describe the plastic behavior of the multilayers as a function of temperature, composition and moisture, and to predict whether or not deformation will be uniform.

1. Introduction

Ethylene-vinyl alcohol copolymer (EVOH) is widely used in high barrier food packages. Packages in which EVOH provides the oxygen barrier are invariably multilayer since EVOH alone does not offer the properties required to make a good monolayer structure. The most significant concern is the sensitivity of the barrier properties to moisture. For this reason, EVOH is multilayered with hydrophobic polyolefins and olefin copolymers [1, 2]. Other advantages to multilayering EVOH with polyolefins include improved processability and heat sealability.

Packaging films are typically drawn at high strain rates. Under these conditions, predictive approaches based only on the properties of the component polymers may not be adequate. A simple rule of mixtures may not apply, especially for describing high strain and failure characteristics, and the film may exhibit mutual reinforcement or alternatively "mutual destruction" [3, 4].

In the present study, the relationship between the mechanical properties of a threelayer film and the component polymers is examined. The multilayer film consists of an ethylene-vinyl alcohol copolymer (EVOH) as the center layer with outer layers of an ethylene-vinyl acetate copolymer (EVA) blend. Plastic deformation at high strain rates is of particular concern. A mathematical model that can be used to predict the deformation characteristics of the multilayer film under relevant process conditions is sought.

2. Experimental

2.1. Materials

A blend of two ethylene-vinyl acetate copolymers and an LLDPE (EVA blend) was used in this investigation. The blend composition was 80% weight of an ethylene-vinyl acetate copolymer (EVA) having 9% mole of vinyl acetate and a melt flow index of 0.3 g/min at 190°C; 10% weight of an EVA characterized by a vinyl acetate molar content of 10% and a melt flow index of 2.2 g/min at 190°C; and 10% weight of a polyethylene (Attane 4201) having a nominal density of 0.910 g/cm^3 and a melt flow index of 1.0 g/min at 190°C. The EVA blend exhibited a melting point of 96°C and had a crystal weight fraction of 23%, based on polyethylene with $\Delta H_f^o = 293$ J/g.

The ethylene-vinyl alcohol copolymer (EVOH) had an ethylene molar content of 38% and a melt flow index of 1.6 g/min at 210°C. Its melting temperature was 176°C and it had a crystalline content of 65 wt%, based on the ΔH_f^o of poly(vinyl alcohol), 117 J/g [5].

*Author to whom all correspondence should be addressed.

TABLE I Volume and layer thickness of EVOH in the multilayers

Volume of EVOH in the multilayer (%)	Thickness of EVOH layer (μm)
1	5
4	20
6	30
8	40
10	50
15	75
20	100

Three layer coextruded films were approximately 0.5 mm thick with EVA blend surface layers and EVOH core layer. Different volume fractions of EVOH were coextruded and are presented in Table I. The reported compositions were determined from the extruder feed ratios.

2.2. Techniques

2.2.1. Dynamic mechanical thermal analysis

Viscoelastic measurements were performed in the tensile mode on a Polymer Laboratories DMTA Mark II instrument. Specimens were about 4 mm wide, 0.5 mm thick and had a gauge length of 15 mm. The DMTA measurements were performed at 1Hz with a heating rate of 4°C/min over the temperature range from −40°C to 140°C.

The water content of EVOH specimens was varied by conditioning specimens for 14 days at room temperature at various relative humidities. Constant relative humidity was obtained with aqueous saturated salt solutions. The salts used were magnesium chloride (34% RH), magnesium nitrate (54% RH), sodium chloride (73% RH), and potassium chloride (86% RH). Dry specimens were obtained by conditioning at room temperature in vacuum for 3 days. The water content was determined by comparing the weight of the conditioned specimen with the dry weight. The ambient laboratory condition corresponded to 54% RH.

2.2.2. Mechanical tensile behavior

Uniaxial tensile experiments were performed in an Instron 8500 hydraulic testing machine equipped with an environmental chamber. Test specimens 50.8 mm wide and 25.4 mm long were tested with a extension rate of 2540 mm/min at temperatures from 55°C to 95°C. The effect of strain rate on the tensile behavior was studied with extension rates from 0.254 mm/min to 254 mm/min. Engineering stress-strain curves were determined from load-displacement data based on the initial specimen geometry.

If the deformation was homogeneous, constant volume during deformation was assumed and the true strain, $\varepsilon_{\text{true}}$, and the true stress, σ_{true}, were calculated by

$$\varepsilon_{\text{true}} = \ln(1 + \varepsilon_{\text{eng}}) \quad (1)$$

$$\sigma_{\text{true}} = \sigma_{\text{eng}}(1 + \varepsilon_{\text{eng}}) \quad (2)$$

where ε_{eng} and σ_{eng} are the engineering strain and the engineering stress, respectively. If the deformation was heterogeneous, i.e., a neck formed and propagated along the specimen axis, the true stress-strain behavior was determined by measuring the local strain in the neck. A 200 Å layer of gold was deposited through an electroformed mesh with 40 wires per inch to obtain a square grid pattern on the gauge portion of the specimen [6]. The image of the grid was recorded continuously during the experiment with a CCD 72 MTI video camera. Assuming constant volume, the true stress and the true strain were calculated by

$$\varepsilon_{\text{true}} = \ln(1 + \varepsilon_l) \quad (3)$$

$$\sigma_{\text{true}} = \sigma_{\text{eng}}(1 + \varepsilon_l) \quad (4)$$

where ε_l is the longitudinal strain of the single mesh length in the neck region. The mesh was monitored along the central axis so that effects of triaxiality in the neck could be neglected [7].

3. Results and discussion

3.1. Ethylene-vinyl acetate (EVA) blend

The EVA blend shows one loss process in the temperature range examined, Fig. 1. This broad β dispersion, from −20°C to 20°C, is associated with the cooperative motions of the glass transition [5]. A gradual decrease in the storage modulus of about 2 orders of magnitude accompanies the β dispersion.

The mechanical behavior of the EVA blend was studied from 55°C to 95°C, the temperature range between the glass transition and the melting point. In this temperature range, the EVA blend deforms homogeneously as indicated by the continuous increase of engineering stress with strain, Fig. 2a. Increasing the temperature decreases the elastic modulus, the post-yield stress level

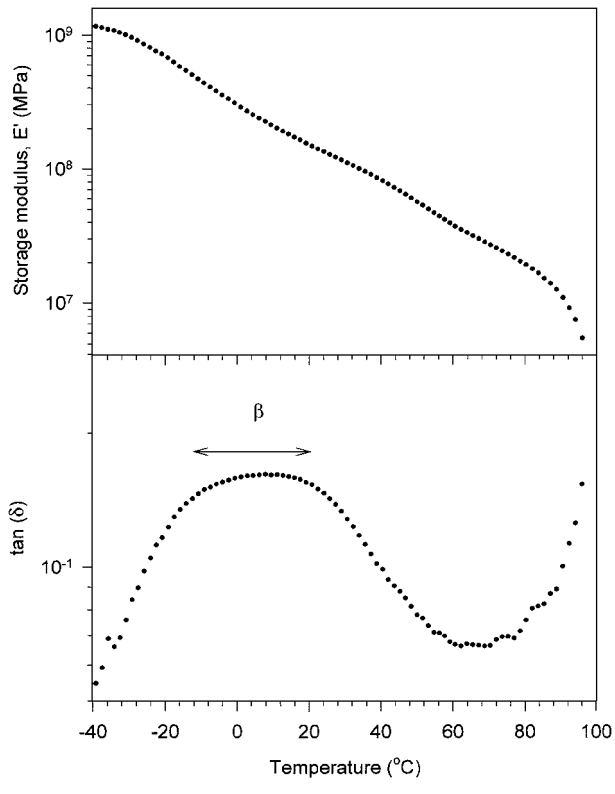

Figure 1 Dynamic mechanical response of the EVA blend.

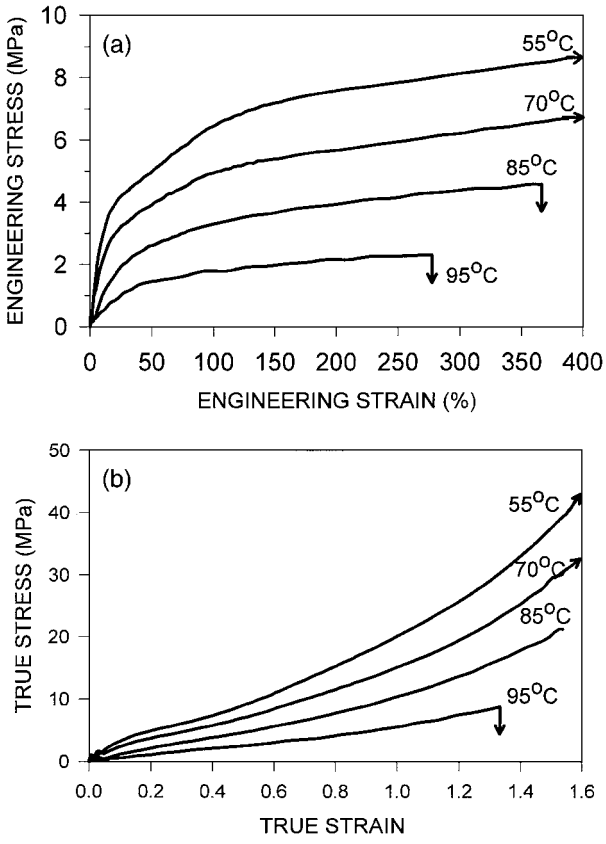

Figure 2 Mechanical behavior of the EVA blend deformed at 2540 mm/min (10,000%/min). (a) Engineering stress-strain curves; (b) true stress-strain curves.

and the fracture strain. Stress-strain curves of vacuum dried specimens were the same as the curves in Fig. 2a, indicating that under ambient conditions of RH, the EVA blend does not sorb sufficient moisture to significantly affect the mechanical properties. The true stress-strain behavior was calculated using Equations 1 and 2 and is illustrated in Fig. 2b. Hardening of the material occurs during plastic deformation, as indicated by the gradual increase of true stress with true strain.

To evaluate the yield stress and the strain hardening parameter of the EVA blend, a model for true stress-strain behavior is required. An empirical constitutive equation of the form

$$\sigma(\varepsilon, \dot{\varepsilon}) = K \exp\left(\frac{\gamma}{2}\varepsilon\right)(\dot{\varepsilon})^m \tag{5}$$

where K is a constant, γ is the strain hardening parameter with a functional dependence $\gamma = \gamma_o\varepsilon$, and m is the strain rate sensitivity, assumed to be strain independent, satisfactorily describes plastic flow of many ductile polymers [8]. If the strain hardening parameter, γ, is strain independent, an alternative expression for the true stress-strain relationship is [9].

$$\sigma(\varepsilon, \dot{\varepsilon}) = \sigma_o(\dot{\varepsilon}) \exp(\gamma\varepsilon) \tag{6}$$

where σ_o is the true yield stress.

According to Equation 6, a plot of ln true stress versus true strain should be linear in the plastic region. Fig. 3a shows true stress-strain data for EVA blend at various temperatures plotted in this manner. The relationship is reasonably linear above a true strain of about 0.4. The intercept and the slope of the linear regression correspond to the true yield stress and the strain hardening parameter, respectively. These values are summarized in Table II. The decrease of the yield stress with temperature reflects the thermally activated nature of yielding. No simple trend is seen for the strain hardening parameter. Fig. 3b compares the experimental true stress-strain data with the calculated curves using σ_o and γ values in Table II. The calculated curves fit the experimental data reasonably well over the range of strains from 0.4 to 1.6. It is clear that Equation 6 describes only the plastic flow behavior of the material, and not the initial low strain region.

TABLE II True yield stress, σ_o, and strain hardening parameter, γ, of EVA blend

Temperature (°C)	σ_o (MPa)	γ
55	4.71	1.41
70	3.87	1.36
85	2.20	1.49
95	1.31	1.42

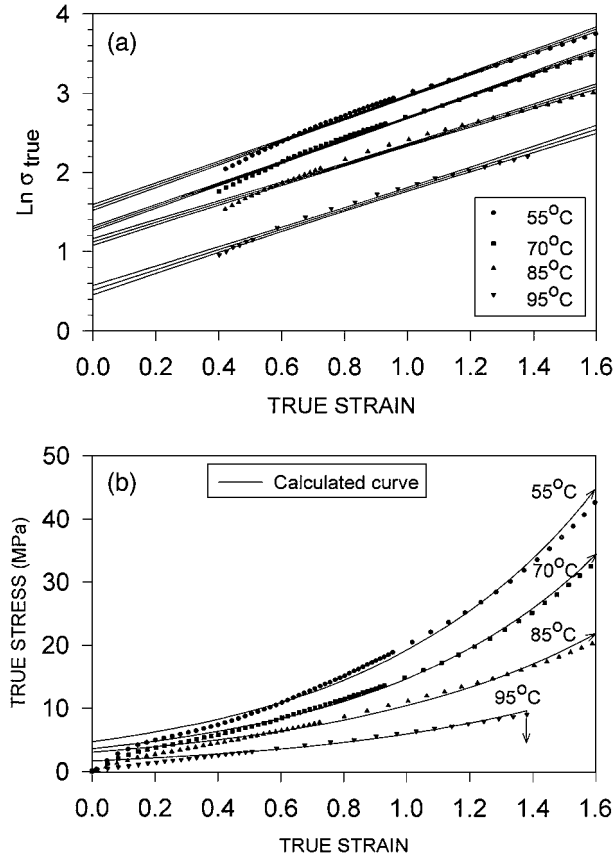

Figure 3 Modeling the true stress-strain curves of the EVA blend deformed at 2540 mm/min (10,000%/min). (a) Ln true stress versus true strain, the 95% confidence range is included with the linear regression; and (b) comparison between experimental data and calculated curves.

3.2. Ethylene-vinyl alcohol copolymer (EVOH)

The dynamic mechanical results for a series of EVOH specimens equilibrated at different RH are presented in

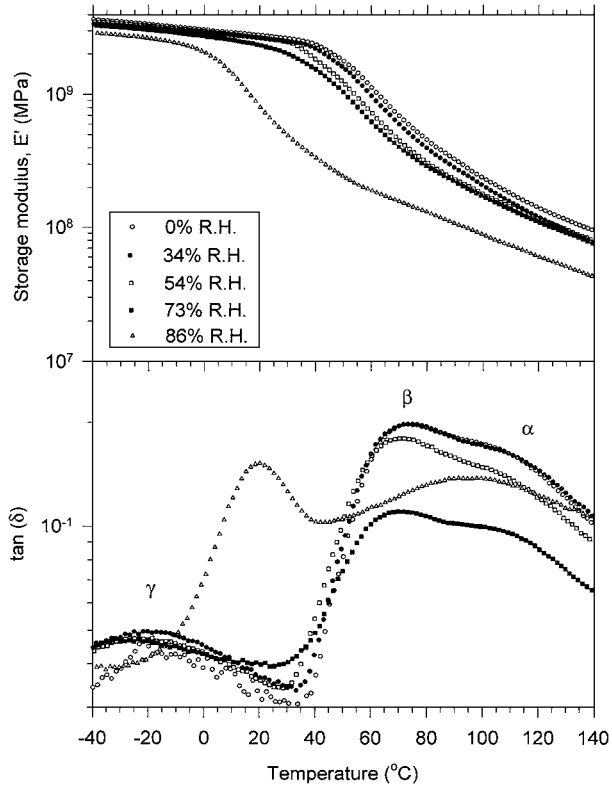

Figure 4 Effect of moisture on the dynamic mechanical response of EVOH.

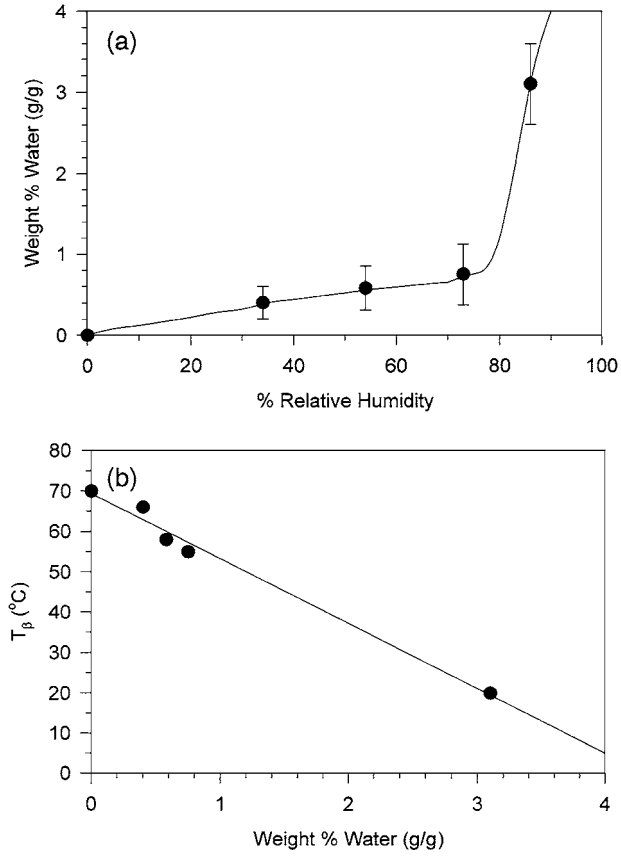

Figure 5 Effect of moisture on EVOH. (a) The sorption isotherm at 23°C; and (b) the effect of moisture content on the glass transition (β transition).

Fig. 4. This material shows three molecular relaxation processes. The α relaxation at about 120°C is attributed to molecular motions in the crystalline phase. The β relaxation, which appears at 70°C for dry EVOH, corresponds to the glass transition. A modulus drop of about an order of magnitude accompanies the β process. The γ relaxation, at about −20°C, is ascribed to large scale molecular motions of non-hydrogen-bonded chains sequences [10]. It will well known that moisture strongly affects the dynamic mechanical behavior of polymers that can hydrogen-bond with water [11, 12]. As the relative humidity increases, the EVOH β process shifts to lower temperatures. This shift is more apparent in the storage modulus than in tan(δ) because of overlap of the α and β tan(δ) peaks.

Fig. 5a summarizes the relationship between relative humidity and water content. Up to 73% RH, the water content gradually increases to about 1%. Between 73% and 86% RH, there is a large increase to about 3%. The linear dependence of the glass transition temperature on water content is illustrated in Fig. 5b. These results show that water acts as a plasticizer for the amorphous phase of EVOH.

The mechanical behavior of EVOH was analyzed in the temperature range that spans the β transition region, 55°C to 95°C. The engineering stress-strain curves for EVOH in Fig. 6 reveal markedly different tensile behavior in terms of yielding and ductility compared to the EVA blend. At all the temperatures, EVOH forms a neck, as indicated by the yield drop. The stress levels are also higher, up to 52 MPa at 55°C. Also in contrast to the EVA blend, the elongation to break increases with the temperature. At 55°C, below the glass transition, a stable neck does not form and fracture occurs just after

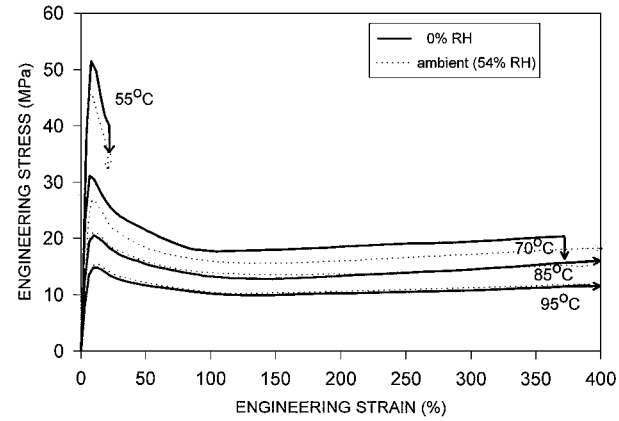

Figure 6 Engineering stress-strain curves of EVOH conditioned at 0% RH and ambient RH (54%), and deformed at 2540 mm/min (10,000%/min).

yielding. At higher temperatures the neck is stable, cold drawing is observed and no fracture is observed up to 400%. An effect of moisture on the tensile behavior of EVOH is observed at 55°C and 70°C. Plasticization by water decreases the yield stress and increases the elongation to break as reported previously in the literature for certain EVOH blends [13].

Neck formation involves an accelerated and localized decrease of the cross-sectional area. An important consequence of necking is the development of true strain rate gradients in the tensile specimen [6, 7]. Before plastic instability, the deformation is uniformly distributed and the true strain is constant along the specimen length. During formation of the plastic instability, the neck

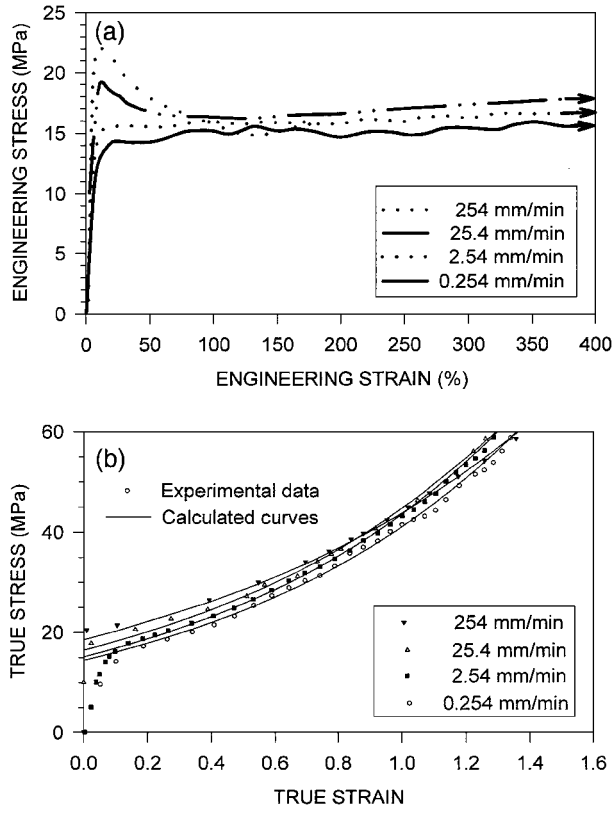

Figure 7 Mechanical behavior of EVOH conditioned at ambient RH (54%) and deformed at 70°C. (a) Engineering stress-strain curves at various extension rates; and (b) the corresponding true stress-strain curves.

region is submitted to a higher true strain rate than the rest of the specimen. If a constant extension rate is used, the true strain rate in the neck region is higher than it would be if the specimen deformed uniformly. This means that EVOH was plastically deformed at a higher strain rate than the EVA blend even though the extension rate was the same.

To determine the true yield stress and the strain hardening parameter of EVOH at the same true strain rate as the EVA blend, it was necessary to examine the effect of strain rate on these parameters. This was done with extension rate lower than 2540 mm/min, the one used to deform EVA blend. The effect of extension rate on the tensile response of EVOH at 70°C is illustrated in Fig. 7a. The deformation mode changes from heterogeneous to homogeneous as the extension rate decreases. The transition occurs between 25.4 mm/min and 2.54 mm/min. The true stress-strain behavior was determined by measuring the local strain during neck

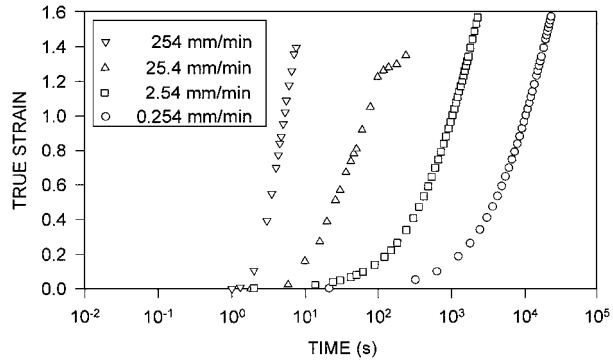

Figure 8 True strain as a function of time for EVOH conditioned at ambient RH (54%) and deformed at 70°C.

formation and applying Equations 3 and 4. Equation 6 described the true stress-strain relationship of EVOH over the range of strains from 0.4 to 1.6, Fig. 7b. Values obtained for the true yield stress and the strain hardening parameter at various strain rates and temperatures are summarized in Table III. As expected, σ_o decreases with increasing temperature and with decreasing strain rate. The strain hardening parameter is essentially independent of temperature but decreases at higher strain rate due to local heating, an effect that is more apparent at the lower temperatures. An increase in the strain hardening parameter with moisture, suggested in Table III, was confirmed by stretching a specimen of EVOH conditioned at 86% relative humidity at 70°C at 254 mm/min. The strain hardening parameter increased from 0.78 (0% RH) to 0.86 (54% RH) to 1.15 (86% RH).

The true strain rate was estimated by constructing a plot of true strain versus time. If deformation was homogeneous, the time was obtained from the extension rate, and the true strain rate was taken as the slope in the strain range of plastic deformation, 0.4 to 1.6 (Fig. 8). When a neck formed, the time was obtained directly from the video recording, and the true strain rate was taken as the highest slope of the true strain versus time curve. The true yield stress and the strain hardening parameter as a function of strain rate are presented in Figs 9 and 10, respectively. The true strain rate of the EVA blend deformed at an extension rate of 2540 mm/min was estimated at 0.6 s^{-1} by this method. The true yield stress of EVOH deformed at the same true strain rate (0.6 s^{-1}) was determined by extrapolation, assuming that ln true yield stress was linearly dependent on ln strain rate. Similarly, a linear regression of the data in Fig. 10 was used to determine the strain

TABLE III True yield stress, σ_o, and strain hardening parameter, γ, for EVOH at 0% and 54% RH at various extension rates and temperatures

		True yield stress (MPa)				Strain hardening parameter			
		Extension rate (%/min) [mm/min]				Extension rate (%/min) [mm/min]			
T (°C)	% RH	1 [0.254]	10 [2.54]	100 [25.4]	1000 [254]	1 [0.254]	10 [2.54]	100 [25.4]	1000 [254]
55	54[a]	18.36	22.31	29.40	–	1.11	1.11	0.89	–
70	54	14.49	15.18	16.44	18.54	1.05	1.06	0.95	0.86
70	0	13.93	16.23	19.98	25.06	1.05	1.07	0.92	0.78
85	54	10.58	11.45	12.04	13.56	1.05	1.05	1.03	0.93
95	54	7.31	8.00	9.30	11.36	1.08	1.08	1.05	0.91

[a]Ambient RH.

TABLE IV True yield stress, σ_o and strain hardening parameter, γ, of EVOH deformed at 0.6 s^{-1}

Temperature (°C)	% RH	σ_o (MPa)	γ
55	54[a]	35.00	0.79
70	54	18.21	0.87
70	0	24.55	0.81
85	54	13.41	0.95
95	54	11.15	0.93

[a]Ambient RH.

TABLE V Strain rate sensitivity, m, for EVOH at 0% and 54% RH at various temperatures

Temperature (°C)	% RH	m
55	54[a]	0.07
70	54	0.03
70	0	0.06
85	54	0.03
95	54	0.04

[a]Ambient RH.

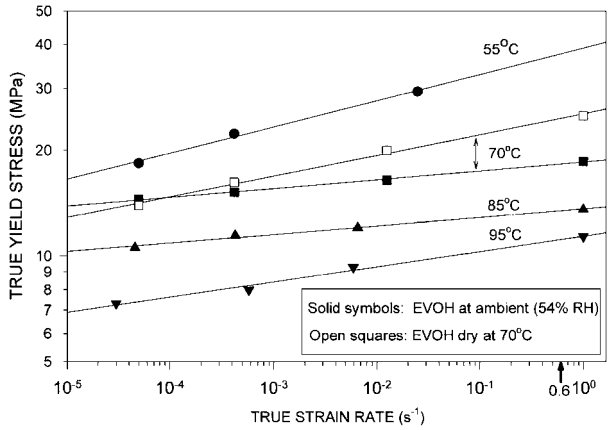

Figure 9 Effect of the true strain rate on the yield stress of EVOH.

hardening parameter at 0.6 s^{-1}. Table IV summarizes the parameters for EVOH deformed at 0.6 s^{-1} at various temperatures. Compared to the EVA blend, EVOH has a higher true yield stress and a lower strain hardening parameter at this true strain rate (see Table II).

The transition from homogeneous deformation to neck formation as the strain rate increases can be explained by considering the general criterion developed by Hart [14]. It is based on the strain hardening parameter (γ), and the strain rate sensitivity (m), of the material and has the form

$$\gamma + m - 1 \geq 0 \tag{7}$$

where the strain hardening parameter is defined as

$$\gamma \equiv \left(\frac{\partial \ln \sigma}{\partial \varepsilon}\right)_{\dot{\varepsilon}}$$

and the strain rate sensitivity as

$$m \equiv \left(\frac{\partial \ln \sigma}{\partial \ln \dot{\varepsilon}}\right)_{\varepsilon}$$

A positive value of $(\gamma + m - 1)$ denotes a stable deformation state and equality is the condition for the transition from a stable to an unstable state. For EVOH, the strain rate sensitivity at the yield point was estimated as the slope of the ln true yield stress versus ln true strain rate plot (Fig. 9). The strain rate sensitivity obtained for EVOH (Table V) is on the same order of magnitude as for other polymers [8] and is 10 times less than the strain hardening parameter. Therefore, according to Equation 7, γ determines whether the material will neck or deform uniformly. The change in the strain hardening parameter from a value greater than 1 at 2.54 mm/min to a value less than 1 at 25.4 mm/min coincides with the observed transition from homogeneous to heterogeneous deformation.

The decrease in the strain hardening of EVOH with increasing extension rate (see Table III), and the consequent transition from homogeneous to heterogeneous

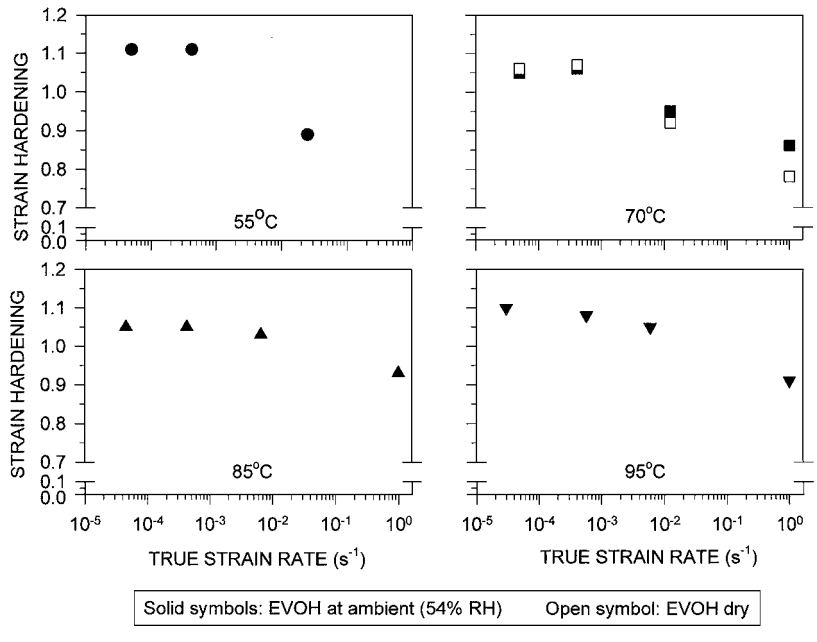

Figure 10 Effect of the true strain rate on the strain hardening parameter of EVOH.

deformation, may occur because isothermal conditions are not maintained at high strain rates [15, 16]. Adiabatic heating at higher strain rates may also affect the EVA blend where the strain hardening parameter decreases from 1.47 to 1.41 when the strain rate increases from 2.54 mm/min to 2540 mm/min. In contrast to EVOH, the strain hardening parameter for EVA blend remains above the critical value of 1 so that deformation is homogeneous over the entire strain rate range.

3.3. EVA blend/EVOH/EVA blend multilayers

Fig. 11 shows the DMTA spectra of the EVA blend/EVOH/EVA blend multilayer containing 20% of EVOH conditioned at ambient RH (54%) and 0% RH. Two major peaks were observed in the loss tangent curves. The peak in the 40°C–80°C range corresponds to the β relaxation of EVOH and the broad peak at lower temperatures results primarily from the glass transition of the EVA blend. The β relaxation of EVOH in the multilayer conditioned at ambient RH is 12°C lower than the β in the dry state. Comparison with the dynamic mechanical analysis of EVOH (Fig. 4) indicates that ambient conditions correspond to 54% RH.

Tensile behavior of the multilayers depends on the composition and water content, as is seen in Fig. 12. The stress level increases with the volume fraction of EVOH and decreases with moisture. The decrease of stress with moisture is more pronounced as the EVOH content increases.

Fig. 13a presents the effect of temperature on the engineering stress-strain curve of the 20% EVOH multilayer conditioned at ambient RH. In the temperature range examined, the multilayer deforms homogeneously, like the EVA blend. None of the specimens had fractured when the experiments were halted at 400% strain. The true stress-strain response was calculated using Equations 1 and 2 and is illustrated for 20% EVOH multilayer in Fig. 13b.

The plot of ln true stress versus true strain is linear above a true strain of 0.4, as is shown in Fig. 14a. Table VI summarizes the parameters obtained for the 20% EVOH multilayer. The values obtained for the true yield stress and the strain hardening parameter are intermediate between those of the individual components

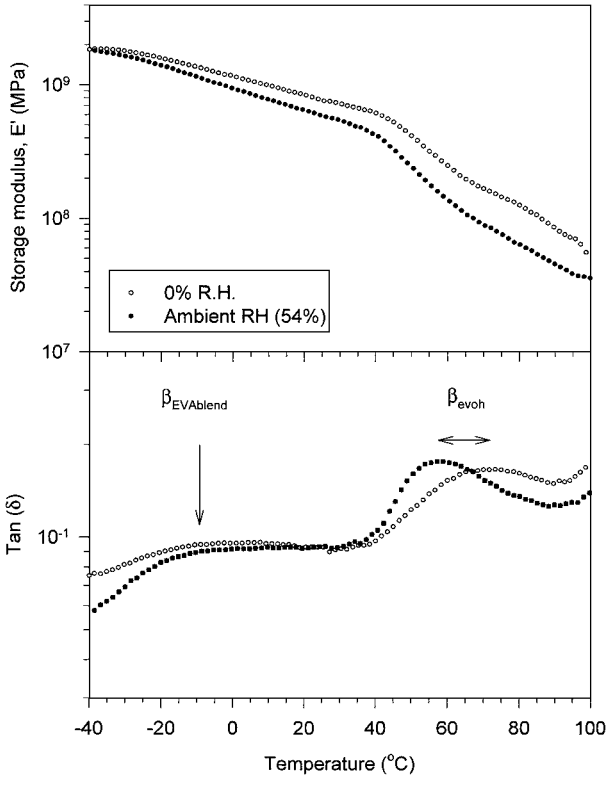

Figure 11 Effect of moisture on the dynamic mechanical response of the multilayer containing 20% EVOH.

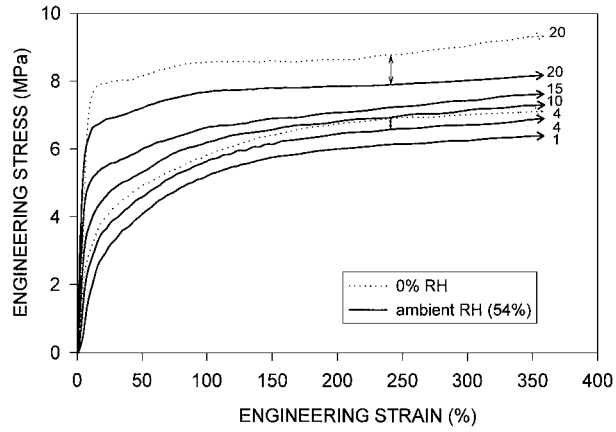

Figure 12 Engineering stress-strain curves of multilayers at 70°C at 2540 mm/min (10,000%/min). The vol% EVOH is indicated. The effect of moisture is illustrated for multilayers containing 4% and 20% EVOH.

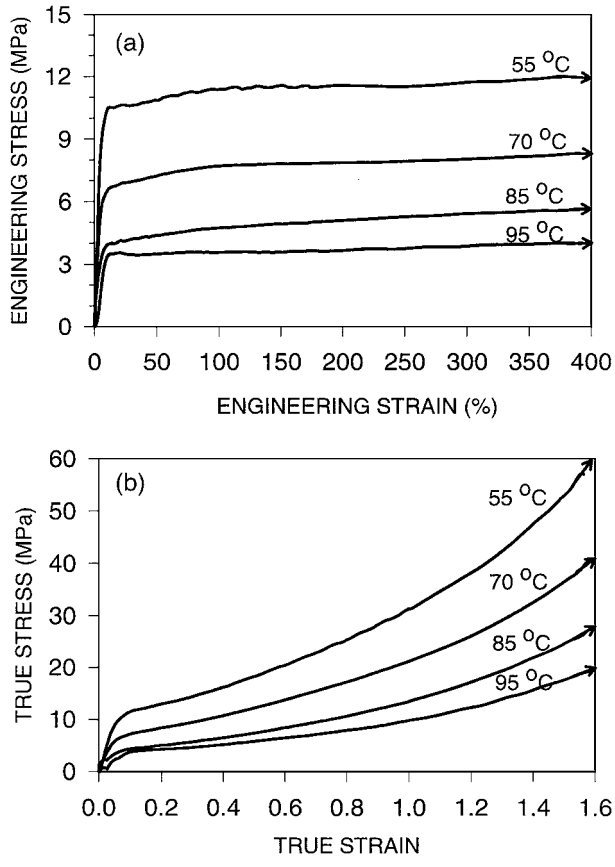

Figure 13 Mechanical behavior of the multilayer containing 20% EVOH conditioned at ambient RH (54%) and deformed at 2540 mm/min (10,000%/min). (a) Engineering stress-strain curves; and (b) true stress-strain curves.

TABLE VI True yield stress, σ_o, and strain hardening parameter, γ, of the multilayer containing 20% of EVOH

Temperature (°C)	σ_o (MPa)	γ
55	10.98	1.06
70	6.87	1.12
85	4.16	1.18
95	3.32	1.09

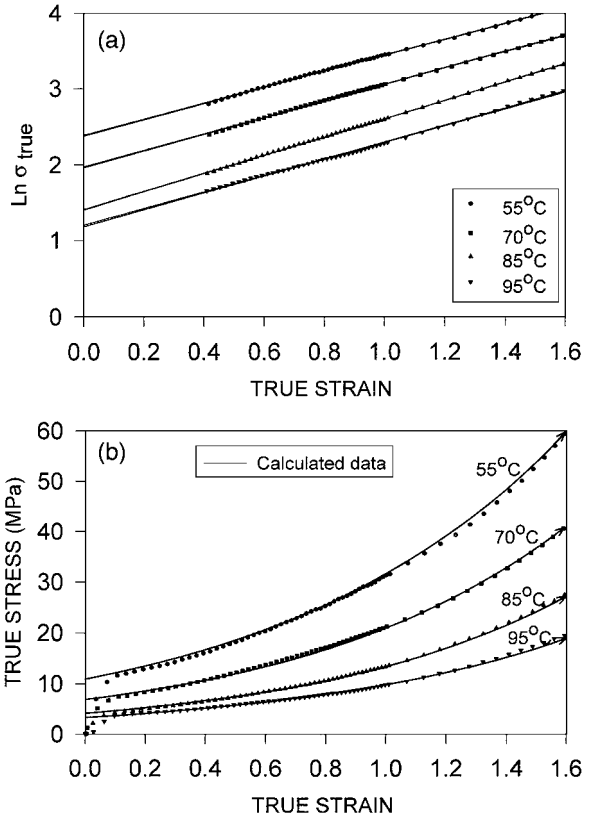

Figure 14 Modeling the true stress-strain curves of the multilayer containing 20% EVOH conditioned at ambient RH (54%) and deformed at 2540 mm/min (10,000%/min). (a) Ln true stress versus true strain; and (b) comparison between experimental data and calculated curves.

(see Tables II and IV). Comparison of the experimental data with the calculated curves in Fig. 14b shows that Equation 6 gives a good description of the plastic behavior of the multilayers.

The true yield stress and the strain hardening parameter of the various multilayers are plotted as a function of EVOH volume fraction in Figs 15 and 16. As the EVOH content increases, the true yield stress increases whereas the strain hardening parameter decreases. Both σ_o and γ are moisture dependent, Fig. 17. The yield stress decreases and the strain hardening parameter increases with the water content.

Qualitatively σ_o and γ of the multilayers follow trends that would be expected based on the behavior of the components. The simplest approach to reconstructing the plastic behavior of the multilayers from the characteristics of the components is to assume a rule of mixtures. The layers in the multilayer structure are considered in parallel. This assumes that the strain and the strain rate are the same in each layer, and the true stress on the multilayer, σ_M, has the form

$$\sigma_M = \alpha\sigma_{EVOH} + (1-\alpha)\sigma_{EVA} \quad (8)$$

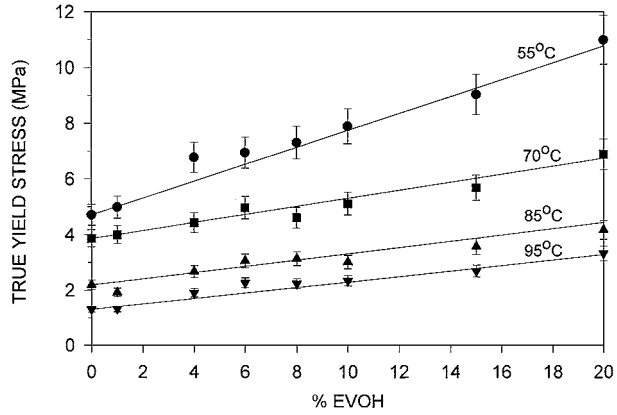

Figure 15 The true yield stress of multilayers conditioned at ambient RH as a function of EVOH content. Symbol represent the experimental data and solid line are calculated according to the rule of mixtures.

where α is the EVOH volume fraction, σ_{EVOH} and σ_{EVA} are the true stresses carried by the EVOH core-layer and the EVA blend surface-layers, respectively. By combining Equation 8 and Equation 6, the true stress-strain relationship of the multilayer is

$$\sigma_{oM}\exp(\gamma_M\varepsilon) = \alpha\sigma_{oEVOH}\exp(\gamma_{EVOH}\varepsilon) + (1-\alpha)\sigma_{oEVA}\exp(\gamma_{EVA}\varepsilon) \quad (9)$$

where σ_{oM}, σ_{oEVOH} and σ_{oEVA} are the true yield stresses of the multilayer, the EVOH layer and the EVA blend layers, respectively; γ_M, γ_{EVOH} and γ_{EVA} are the strain hardening parameters of the multilayer, the EVOH layer and the EVA blend layers, respectively. From Equation 9, it is possible to describe the true yield stress, σ_{oM}, and the strain hardening, γ_M, as a function of the parameters of the components:

$$\sigma_{oM} = \alpha\sigma_{oEVOH} + (1-\alpha)\sigma_{oEVA} \quad (10)$$

and

$$\gamma_M(\varepsilon) = \frac{\partial \ln\sigma_M}{\partial\varepsilon} = \frac{\partial \ln[\alpha\sigma_{oEVOH}\exp(\gamma_{EVOH}\varepsilon) + (1-\alpha)\sigma_{oEVA}\exp(\gamma_{EVA}\varepsilon)]}{\partial\varepsilon} \quad (11)$$

The parameters σ_{oM} and γ_M were calculated for a true strain rate of 0.6 s^{-1} by using the parameters of the components in Tables II and IV. The temperature, composition, and moisture dependencies of σ_o and γ obtained by this calculation are included in Fig. 15 to Fig. 17 as the solid lines. The good correlation between the measurements and calculations shows that the rule of mixtures can be used to obtain the plastic behavior of the multilayers. Good adhesion between EVOH and EVA blend layers ensures that they deform at the same true strain rate in the multilayer. At 0.6 s^{-1}, EVOH without the EVA layers would neck because γ is lower than unity (Table IV). Whether deformation of the multilayers is homogeneous or heterogeneous is determined by the composite strain hardening parameter in accordance with Equation 7. As long as EVA controls the

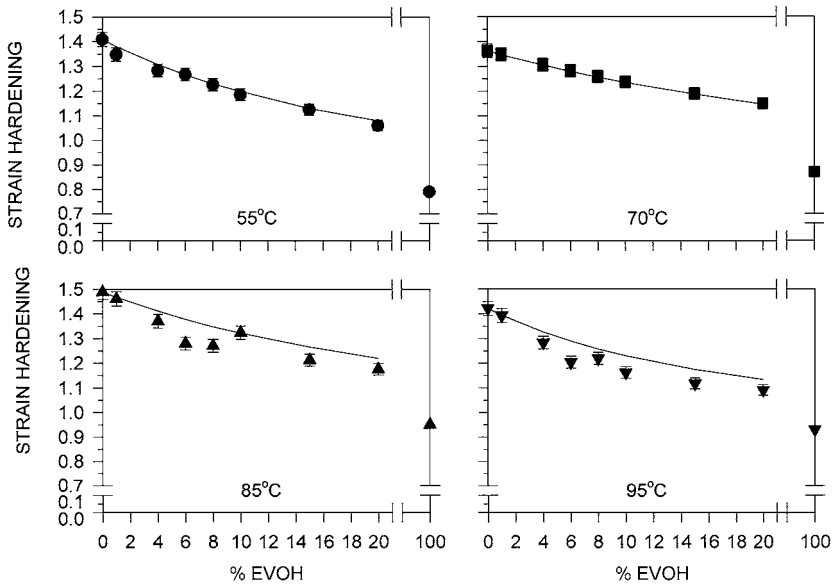

Figure 16 The strain hardening parameter of multilayers conditioned at ambient RH as a function of EVOH content. Symbols represent the experimental data and solid lines are calculated according to the rule of mixtures.

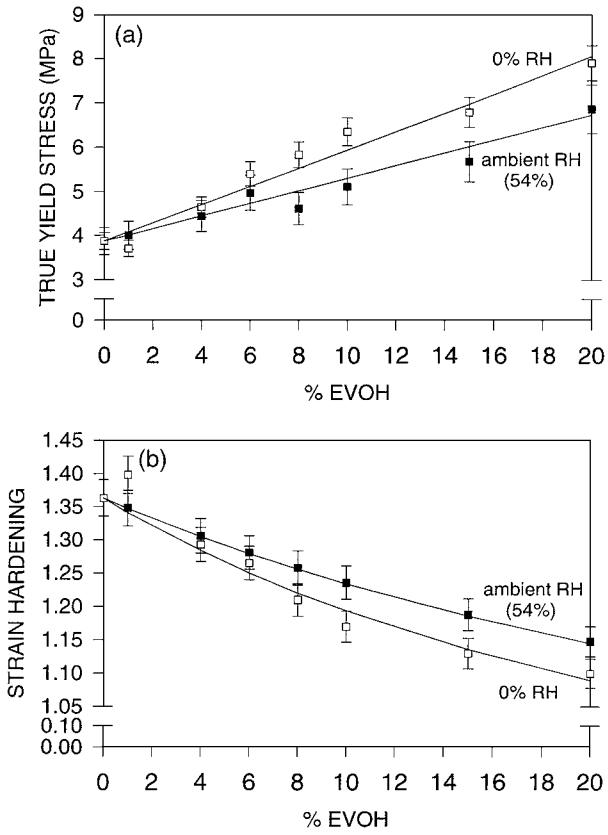

Figure 17 Effect of moisture on the mechanical parameters of EVOH deformed at 70°C. (a) The true yield stress; and (b) the strain hardening parameter. Symbols represent the experimental data and solid lines are calculated according to the rule of mixtures.

deformation, the multilayer will deform uniformly at high strain rates. For all the compositions examined, this was the case: γ_M was greater than unity and deformation was uniform. It is possible to predict conditions at which the transition from homogeneous deformation to neck formation will occur. For example, at 55°C and ambient RH, it is anticipated that microlayers containing more than 30% EVOH will form a neck.

4. Conclusion

This investigation of the plastic deformation of EVA blend/EVOH/EVA blend multilayers at high strain rates leads to the following conclusions:

1. Individually, the components exhibit very different deformation characteristics at the temperatures and strain rates studied. The EVA blend deforms uniformly in contrast to the EVOH which necks at high strain rates.

2. Plastic deformation of the components and the multilayers is satisfactorily described by a true stress-strain relationship with two parameters, the true yield stress and the strain hardening parameter. Moisture acts as a plasticizer for EVOH, and causes the yield stress to decrease and the strain hardening parameter to increase.

3. The composite true yield stress and strain hardening parameter obtained by a simple rule of mixtures approach make it possible to calculate the plastic true stress-strain behavior of the multilayer as a function of temperature and composition, and to predict whether or not deformation will be uniform.

Acknowledgements

The authors gratefully acknowledge the generous financial support provided by Pechiney Recherche, Paris, France.

References

1. B. C. TSAI and J. A. WATCHEL, "Barrier Polymers and Structures," edited by W. J. Koros (ACS Symp. Series 423, Washington, DC, 1990) p. 192.
2. M. M. ALGER, T. J. STANLEY and J. DAY, "Barrier Polymers and Structures," edited by W. J. Koros (ACS Symp. Series 423, Washington DC, 1990) p. 203.
3. W. J. SHRENK and T. ALFREY, JR., *Polym. Eng. Sci.* **9** (1969) 393.
4. B. L. GREGORY, A. SIEGMANN, J. IM, A. HILTNER and E. BAER, *J. Mater. Sci.* **22** (1987) 532.
5. A. APICELLA, H. B. HOPFENBERG and S. PICCAROLO, *Polymer Eng. Sci.* **22** (1992) 382.

6. S. NAZARENKO, S. BENSASON, A. HILTNER and E. BAER, *Polymer* **35** (1994) 3883.
7. C. G'SELL, N. A. ALY-HELAL and J. J. JUKES, *J. Mater. Sci.* **18** (1983) 1731.
8. C. G'SELL and J. J. JONAS, *ibid.* **14** (1979) 583.
9. S. BAHADUR, *Polym. Eng. Sci.* **13** (1973) 266.
10. M. L. ADDONIZIO, L. D'ORAZIO and E. MARTUSCELLI, *ibid.* **28** (1993) 3793.
11. Y. S. PAPIR, S. KAPUR, C. E. ROGERS and E. BAER, *J. Polym. Sci. Part A-2* **10** (1972) 1305.
12. A. HILTNER, *Polym. Eng. Sci.* **19** (1979) 722.
13. P. A. DELL and W. G. KOHLMAN, *J. Appl. Polym. Sci.* **52** (1994) 353.
14. E. W. HART, *Acta Metall.* **15** (1967) 351.
15. J. M. ANDREWS and I. M. WARD, *J. Mater. Sci.* **5** (1970) 411.
16. A. MARQUEZ-LUCERO, C. G'SELL and K. W. NEALE, *Polymer* **30** (1989) 636.

Received 26 September 2001
and accepted 28 February 2002